Leading-Edge Vortex Dynamics on a Slender Oscillating Wing

Young-Whoon Jun* and Robert C. Nelson†
University of Notre Dame, Notre Dame, Indiana

Experimental data are presented which show the dynamic behavior of the leading-edge vortices on an 80-deg swept delta wing undergoing a wing rock motion. The experiments were conducted in a low-speed wind tunnel, and the model Reynolds number was 315,000, based on the centerline chord. Vortex trajectory data were determined from smoke flow visualization experiments. The photographic data were analyzed to determine vortex position and breakdown information. Significant differences were observed between the static and dynamic vortex core positions and the breakdown locations. The data show the convective lag in the flowfield development on a wing oscillating in roll.

Introduction

AN interesting example of the importance of unsteady aerodynamics is a self-induced roll oscillation known as wing rock. Wing rock can occur at high angles of attack for aircraft with highly swept wing planforms. Such oscillations lead to a significant loss in average lift, which can cause a serious safety problem for the aircraft during maneuvers such as landing. In addition, the wing rock motion restricts the performance envelope of aircraft exhibiting this behavior.

Several theories have been developed to explain the wing rock phenomenon. Analytically, it has been shown that a limit cycle rolling motion can be produced by either static nonlinear aerodynamics, loss of roll damping, or aerodynamic hysteresis.[1-5] Each of these aerodynamic nonlinearities has been observed experimentally in wind-tunnel tests for slender aircraft models at large angles of attack. Which mechanism or combination of aerodynamic characteristics causes the wing rock motion is still unclear.

An interesting explanation of the fluid mechanic mechanisms causing the wing rock motion of slender wings was developed by Ericsson.[5] In his analysis, he shows that wing rock is caused by the asymmetry of leading-edge vortices. To explore the effect of sideslip and roll angle on the motion of slender delta wings, Ericsson defines an effective apex half-angle for the right and left halves of the wing. For small angles, i.e., $\beta \leq 15$ deg and $\theta_A \leq 15$ deg, the effective half-angle can be expressed as

$$\bar{\theta}_A = \theta_A + \Delta\theta_A$$

where $\bar{\theta}_A$ is effective semiapex angle and $\Delta\theta_A$ is the apparent change in semiapex half-angle due to the rolling motion of the model. The apparent change in semiapex angle can be expressed as a function of the angle of attack and sideslip angle as follows:

$$(\Delta\theta_A)_{RL} = \pm\tan\alpha_o \sin\phi = \pm\beta/\cos\alpha_o$$

where α_o is the angle of attack, ϕ the roll angle, and β the angle of sideslip. As the model rolls about its longitudinal axis, a sideslip angle is created. The resulting sideslip angle causes an effective decrease of the sweep angle (increase of the semiapex angle) on the downward portion of the wing while the upward wing experiences an effective increase in sweep angle (decrease in semiapex angle). The plus and minus sign in the preceding equation refers to the right and left sides of the wing, respectively. Using this simple formula and the static data on vortex asymmetry and breakdown from Ref. 6, which is reproduced in Fig. 1, Ericsson showed that vortex asymmetry can cause wing rock motion but that vortex breakdown cannot.

For example, if the model has an angle of attack and semiapex half-angle as illustrated in Fig. 2a, then the model will begin to roll in a clockwise direction if the vortex asymmetry is as indicated in the middle sketch. As the model rolls, the effective semiapex angle on the downward-moving portion of the wing increases. As the effective semi-apex angle increases, the right vortex will try to assume the symmetric position while the left side will experience a decrease in the effective semi-apex angle, which favors vortex liftoff. The switching of the vortex asymmetry creates an effective aerodynamic spring to produce the roll oscillation. A similar argument can be made for the oppositely disposed vortex arrangement.

Ericsson used Fig. 2b to show that vortex breakdown cannot cause the wing rock motion. If the wing conditions are such that vortex breakdown can occur as shown by the middle sketch, then the wing will begin to roll in a clockwise manner. The downward-moving wing will experience an effective increase in the semi-apex angle, which favors vortex breakdown. The breakdown position will move closer to the apex, thereby diminishing the lift on the downward side of the wing. On the other hand, the effective semi-apex angle on the upward-moving portion of the wing will decrease. This favors the movement of the breakdown position away from the apex, which results in an increase in lift on the upward-moving wing portion. The net

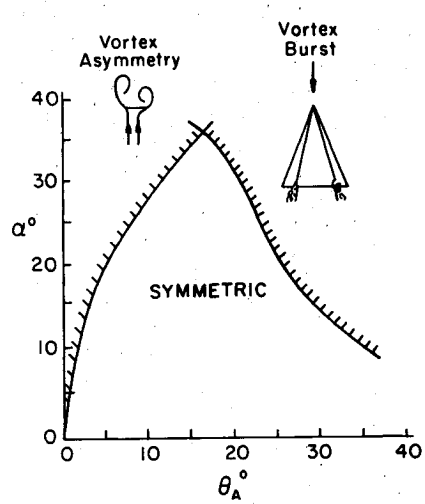

Fig. 1 Boundaries for vortex asymmetry and breakdown.[6]

Presented as Paper 87-0332 at the 25th AIAA Aerospace Sciences Meeting, Reno, NV., Jan. 12–15, 1987; received Aug. 10, 1987; revision received Sept. 18, 1987.

*Postdoctoral Fellow, Department of Aerospace and Mechanical Engineering.

†Professor, Department of Aerospace and Mechanical Engineering. Associate Fellow AIAA.

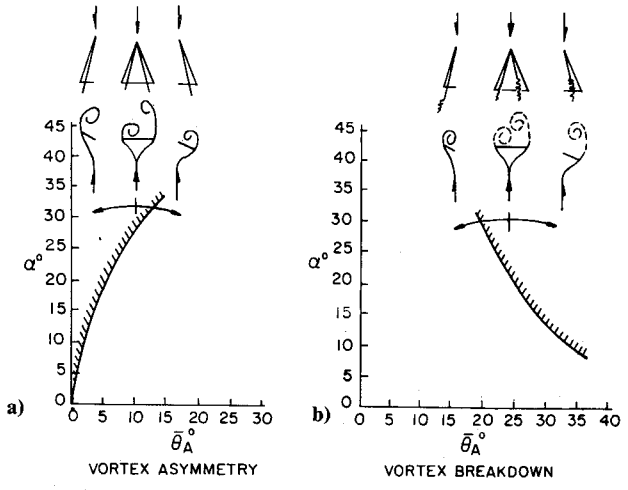

Fig. 2 Effect of vortex asymmetry and breakcown on the wing rock motions[5]: a) Vortex asymmetry; b) Vortex breakdown.

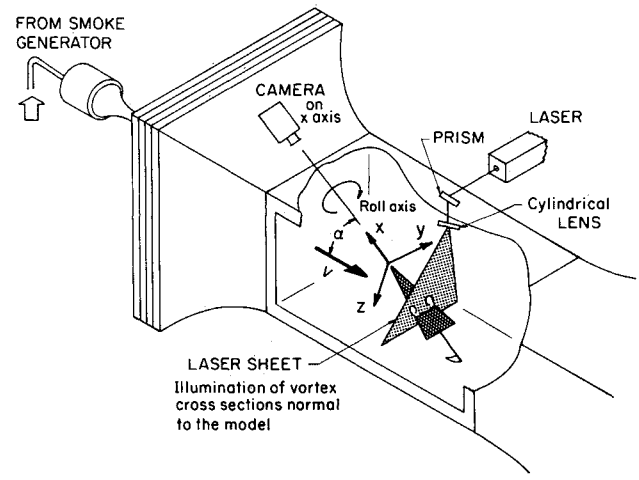

Fig. 3 Sketch of experimental setup.

result is a rolling moment that tends to continue the rolling motion. From this, Ericsson concludes that the roll moment caused by vortex breakdown is destabilizing and would not provide the needed aerodynamic spring to create an oscillation.

Several experimental studies dealing with slender delta wings have provided some insight into the possible flow mechanisms contributing to wing rock motion.[7,8] Two of the more recent studies will be reviewed here. Nguyen et al. conducted an experimental study using an 80-deg leading-edge sweep flat delta wing having a root chord of 5.8 ft.[7] The model was mounted in such a way that the axis of rotation was two inches below the midspan chord. They found the maximum amplitude and period of the motion to be 34 deg and 0.98 s, respectively. They postulated that the wing rock phenomenon is caused by dependence of aerodynamic damping in roll on sideslip such that negative (unstable) roll damping is obtained at the smaller sideslip angles and positive (stable) roll damping is obtained at the larger angles. The displacement of the leeward vortex from the surface of the upgoing side of the wing is a critical factor in that it is the primary mechanism that provides the static restoring moment and the variation in roll damping that causes the wing rock.[7]

A similar experiment was also conducted by Levin and Katz.[7] They tested two wing planforms having leading-edge sweeps of 76 and 80 deg. However, only the wing with the 80-deg sweep would undergo periodic self-induced roll oscillation.They had their axis of rotation on the midspan chord. In order to make the axis of rotation coincide with midspan chord, they housed the bearing assembly inside a rather large hump or bulge along the centerline of the wing. In these experiments, Levin and Katz observed an amplitude of approximately 30 deg and a period of 0.4 s for an angle of attack of 30 deg. They postulated that a wing rock condition can develop when the work done during the roll cycle by destabilizing vortex interactions overcomes the energy dissipation of the wing damping forces. When the wing damping moment is increased as a result of higher aspect ratio or higher angle of attack, the oscillations will be terminated.[8]

The experiments and analysis reported in the cited references provide some insight into the aerodynamic characteristics of the wing rock phenomenon. However, these experiments provide very little data on the unsteady flowfield associated with the rolling motion. The purpose of this paper is to present the results of some preliminary experiments to identify the leading-edge vortex behavior on a delta wing model undergoing a wing rock motion. This is accomplished by a series of flow visualization tests on an 80-deg swept delta wing model that was free to roll about its longitudinal axis.

Experimental Apparatus

A delta wing model with an 80-deg leading-edge sweep was used in these preliminary experiments. The model was 0.049 cm (0.25 in.) thick, has a 6.6-cm (16.8-in.) chord, and an aspect ratio of 0.70. The leading edge was beveled with a 25-deg angle so that a sharp edge was formed on the upper side of the model. The model was mounted on the sting, which permitted the model to roll freely about a bearing system located in the sting support. No attempt was made to measure the damping in the bearing system. The mount also allowed for the variation of angle of attack from 20–40 deg in 5-deg intervals. The tests were conducted in Notre Dame's low-turbulence 0.61-by-0.61-m (2-by-2-ft) wind tunnel. Additional information on the wind tunnel and smoke generating system can be found in Ref. 9. Both still and high-speed motion pictures of the vortex trajectories were obtained. The visualization data were obtained by using smoke and a laser light sheet to illuminate the vortices at three stations along the model. Stations 1, 2, and 3 were located at 1/4, 1/2, and 3/4 of the centerline chord from the apex, respectively. The vortex cross sections were illuminated by passing the laser beam through a cylindrical lens to create a thin sheet of light. Both still and motion picture cameras were positioned so that their field of view was along the longitudinal axis of the model. The high-speed moving pictures (128 frames per s) enable the acquisition of vortex data throughout several wing rock cycles. Figure 3 is a sketch showing the experimental setup.

The photographic records of the model and vortex motions were reduced using a digitizing tablet connected to a microcomputer. The image projected from the film was reflected through a precision front surface mirror and on to the digitizing graphics tablet. The position of the wing tips and vortex core positions were recorded using the stylus of the digitizing tablet. This information was stored in the computer and later reduced to roll angles and nondimensional vortex displacements. The vortex trajectory data are presented in a reference frame fixed to the wing. The axis system is shown in Fig. 3.

The accuracy of the measurements was assessed, and it was determined that the roll angle could be estimated from the photographic records to within ± 0.5 deg. Points on the photographs could be determined to within ± 0.05 in. The vortex core region was identified by the void in the smoke pattern. Locating the center of the vortex introduced additional uncertainty into the measurement. When vortex breakdown occurred, there was no distinguishable point to locate. The centroid of the vortex smoke pattern was assumed to be the vortex center for the vortex after breakdown occurred. Although static and dynamic data were obtained at three chordwise positions along the wing, only the data at station 3 ($x/c_r = -3/4$) are presented in this paper.

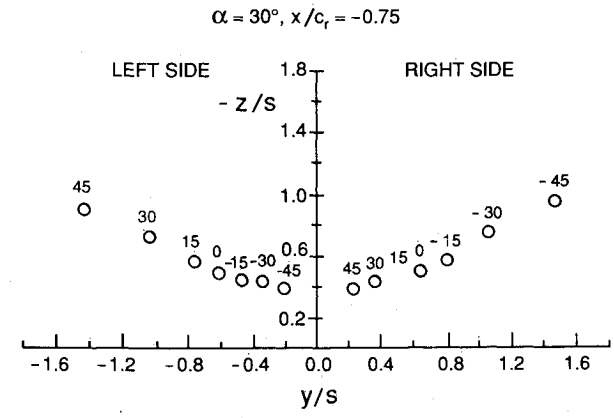

Fig. 4 Static vortex core position data as a function of roll angle ($\alpha = 30$ deg, $x/c_r = -0.75$).

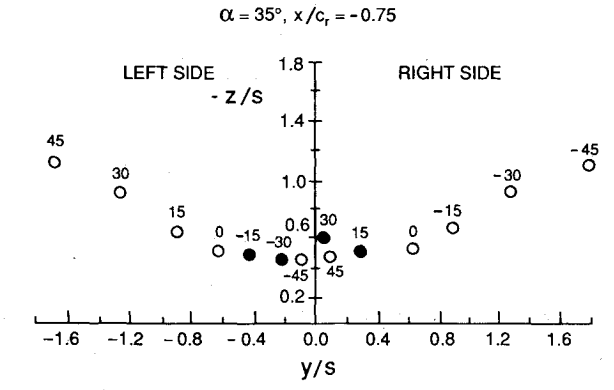

Fig. 5 Static vortex core position data as a function of roll angle ($\alpha = 35$ deg, $x/c_r = -0.75$). Solid symbols indicate that vortex breakdown has occurred.

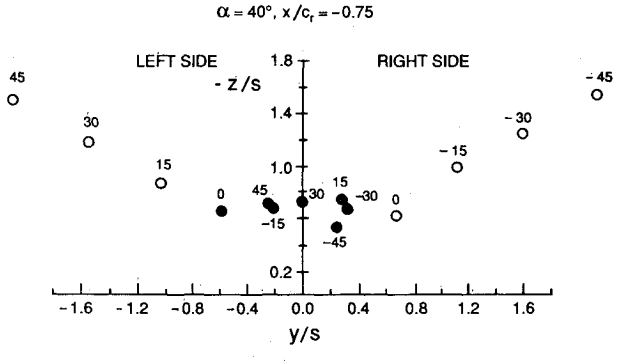

Fig. 6 Static vortex core position data as a function of roll angle ($\alpha = 40$ deg, $x/c_r = -0.75$). Solid symbols indicate that vortex breakdown has occurred.

Results

Both static and free-to-roll tests were conducted using a single-degree-of-freedom roll mechanism. The model was carefully aligned so that it was at zero sideslip at the zero roll angle position. The experiments were conducted at a tunnel speed of 11.3 m/s (37 ft/s), which corresponds to a Reynolds number of 315,000 based upon the model root chord.

Static Data

Measurement of the static vortex position was determined for angles of attack of 30, 35, and 40 deg at the three locations along the model and for roll angles of 0, ±15, ±30, and ±45 deg. A clockwise rotation of the model when viewed from the rear is a positive roll angle. The trajectory data are presented in nondimensional form in a wing fixed frame. Both the vertical and lateral displacements from the wing surface are normalized with respect to the local value of the semispan of the wing. Figures 4–6 show the static measurements for station 3 for different angles of attack.

For positive roll angles (right wing down), the right vortex moves inboard and closer to the model surface while the left vortex moves outboard and farther away from the wing surface. The reverse orientation of the core positions occurs for negative roll angles.

As the angle of attack was increased, vortex breakdown was observed to occur on the model. At 35-deg angle of attack, vortex breakdown occurred at station 3 for the vortex on the downward or windward side of the wing at roll angles of 15, 30, −15, and −30, but not at the ±45-deg roll angle. These data are shown in Fig. 5. When the angle of attack was increased to 40 deg, vortex breakdown occurred at stations 2 and 3. At station 2, vortex breakdown occurred at roll angles of 15, 30, −15, and −30 deg for the vortex on the downward or windward side of the wing, but at station 3, vortex breakdown occurred at all roll angles on the downward side of the wing even at zero roll angle, as shown in Fig. 6. Vortex breakdown positions were observed to move back and forth depending upon the roll angle. The vortex breakdown positions move forward when roll angles are between ±15 and ±30 deg and then move downstream when the absolute value of roll angle is greater than ±30 deg. It was noticed that even at zero roll angle, vortex breakdown occurred only on the left side, which means the flow pattern was asymmetric for the model.

A sequence of photographs is presented in Fig. 7 that shows the leading-edge vortices on the stationary model. The flow pictures are for station 3 when the model is at 35-deg angle of attack. The roll angle was varied in 15-deg increments from 0–45 deg. Vortex breakdown occurred on the down or windward side of the wing as the wing roll angle increased to 15 and 30 deg, respectively. However, when the wing is at roll angle of 45 deg, the breakdown position has moved aft of station 3. Initially, the breakdown position on the downward side of the wing was observed to move forward toward the apex as the roll angle was increased and then began to move aft and off the wing for large roll angle. When vortex breakdown occurs on the downward portion of the wing, the lift on the lower wing is reduced, and the contribution of the vortex lift to the roll-restoring moment is diminished. However, at large roll angles, the breakdown position moves off the wing, thereby increasing the vortex lift and the restoring moment contributed by the downward portion of the wing. The reason for the change in direction of vortex breakdown position with roll angle is not clear at this time. One possible explanation for the change is as follows. As the model is rolled, the effective sideslip angle that is created increases with increasing roll angle. It is well-known that as the sideslip angle increases, the breakdown position on the windward side of the wing will move toward the apex. On the other hand, the effective angle of attack of the wing decreases with increasing roll angle, which favors movement of the vortex breakdown position away from the apex. It would appear that at some intermediate roll angle, the favorable effect on vortex breakdown due to the effective reduction in angle of attack is greater than the unfavorable effect due to sideslip.

Dynamic Data

After the static measurements were completed, the model was allowed to rotate freely about its roll axis. A typical plot of the roll time history of the wing rock motion is shown in Fig. 8. The motion is an undamped sinusoidal oscillation having a maximum roll amplitude of 53 deg and a frequency of 2.17 cycles/s. For the dynamic tests, the vortex position data were found to differ from the static data. In addition, it was observed that the vortex position for a given roll angle depended upon the direction in which the model was rolling. Figure 9 is a sketch showing a complete cycle of the roll oscillation and the vortex trajectory at a given station along the wing. For convenience in viewing the data, the individual sketches of the model are presented so that one can view a given roll angle magnitude

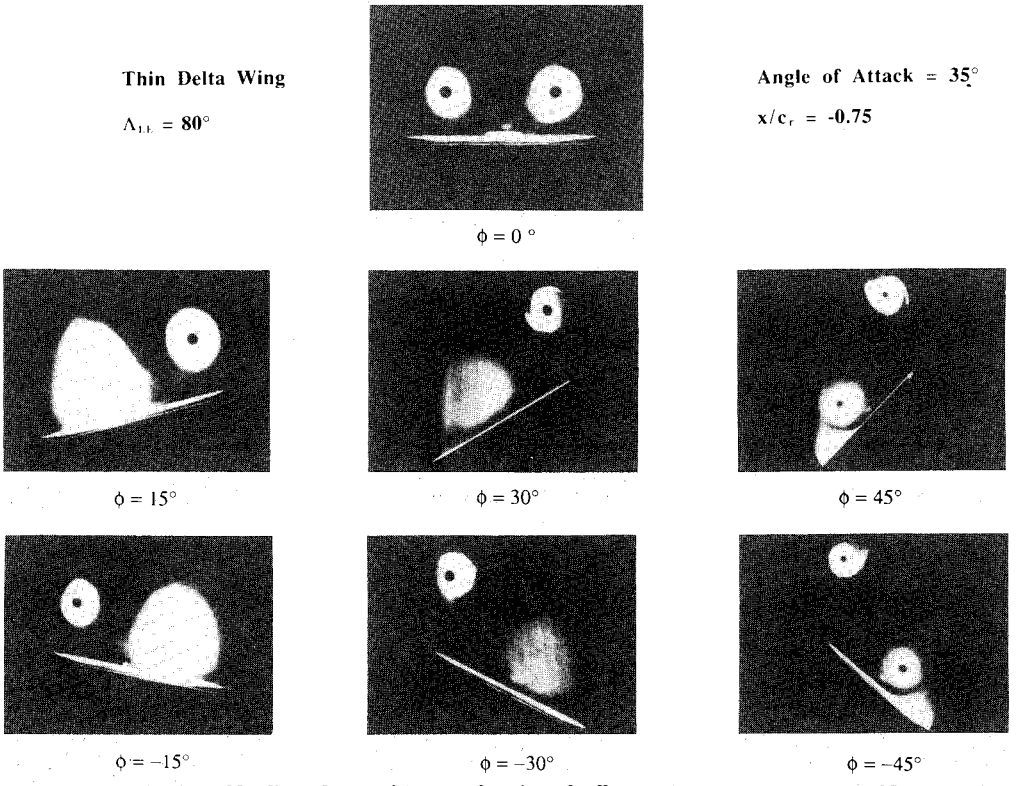

Fig. 7 Flow visualization of leading-edge vortices as a function of roll angle (stationary model, $\alpha = 35$ deg, station 3).

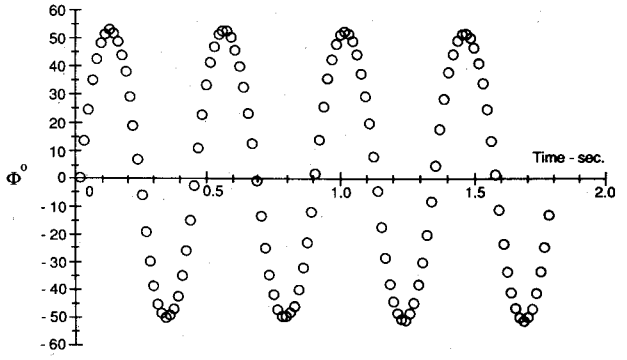

Fig. 8 Roll angle time history ($\alpha = 30$ deg, $\phi_{max} = 53$ deg, $f = 2.17$ cycles/s).

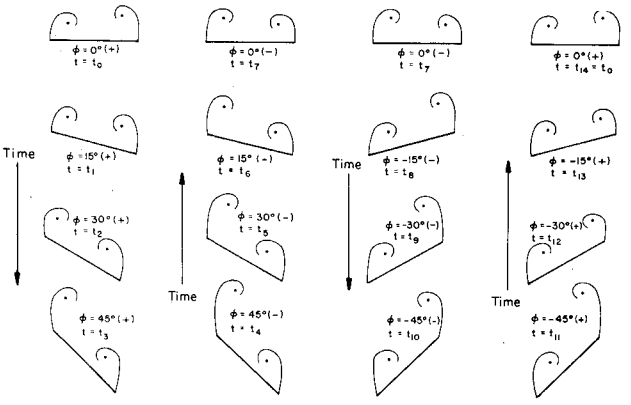

Fig. 9 Sketch of vortex trajectories in one cycle of the wing rock motion.

by looking across the figure. The time scale is indicated by the direction of the arrows to the left of the individual sketches.

In looking across the chart, we see that at a given roll angle the position of the vortices depends upon the direction of the rolling motion. For example, at $\phi = \pm 15$ deg, the relative positions of the vortices are quite different, depending upon whether the model is rolling in the positive or negative direction. It is interesting to note, however, that the vortex positions are the mirror images of one another at plus or minus a given angle when the roll rate is in the same direction.

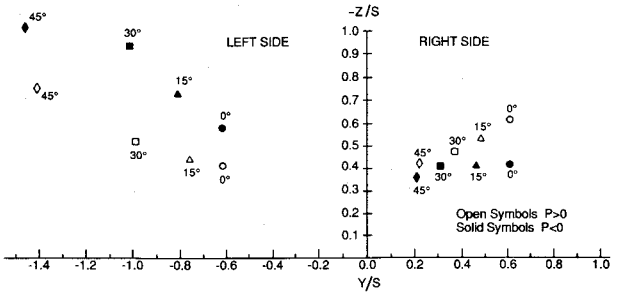

Fig. 10 Dynamic vortex core position data ($\alpha = 30$ deg, $x/c_r = -0.75$).

In looking down the first column, we see that the right vortex is initially higher than the left vortex. This asymmetry causes the model to start to roll in the clockwise or positive sense. As the model rolls, the left vortex begins to move outboard and away from the upper surface of the model, while at the same time the right vortex is moving inboard and closer to the model upper surface. During this portion of the cycle, the roll moment, which was positive at the start of the motion, becomes negative, causing the model eventually to reverse its direction of rotation. Similar arguments can be made for the remaining portion of the cycle.

Figure 10 shows the position data of the right and left vortices at positive roll angles for either positive or negative roll rates. The difference in vortex position is greatest on the left side of the wing, which is always above or equal to the horizontal plane. The larger vertical displacement occurs when the wing is rolling in a direction away from the vortex, and the lower measurements are for the case when the wing surface is moving toward the vortex. These data clearly illustrate the lag

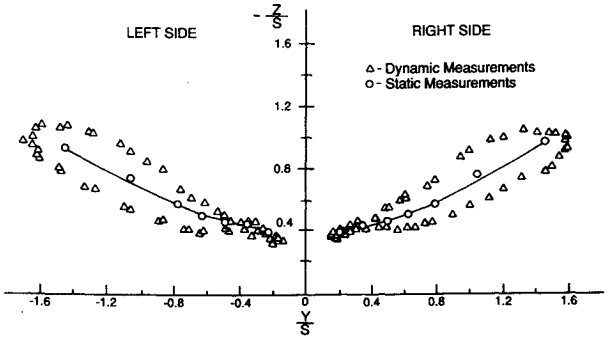

Fig. 11 Comparison of dynamic and static core position data ($\alpha = 30$ deg, $x/c_r = -0.75$).

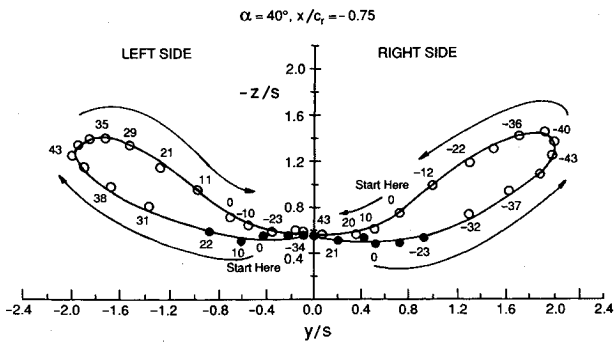

Fig. 12 Dynamic vortex core position data for one complete cycle ($\alpha = 40$ deg, $x/c_r = -0.75$). Solid symbols indicate that vortex breakdown has occurred.

in the flowfield development. Numerical simulations made by Konstadinopoulos et al[10] using an unsteady vortex-lattice model to determine the vortex trajectories predict a similar trend in the dynamic behavior of the vortices. These results also indicate that the vortex asymmetry provides an aerodynamic spring.

Figure 11 shows the trajectory data for several cycles of the wing rock motion for the 30-deg angle of attack at station 3. The static data are included for comparison and were found to lie between the dynamic curves. Figure 12 shows the vortex core trajectories as a function of the roll angle for an angle of attack of 40 deg for one complete cycle. The roll angle has been annotated on the figure to illustrate the flowfield lag. Vortex breakdown occurred only at 40-deg angle of attack and at station 3. This phenomenon is different from that of the static condition. Under static conditions, vortex breakdown was found to occur at 35- and 40-deg angles of attack at station 2 for roll angles of ± 15 and ± 30 for the downward wing vortex and at station 3 for all roll angles. Although vortex breakdown does not of itself cause the wing rock motion, it does appear to play a more important part in the wing rock motion than has been suggested in previous studies. Furthermore, when breakdown occurs, the other vortex is displaced outboard and upward, which affects its influence on the wing's aerodynamic roll characteristics.

Concluding Remarks

The experiments reported in this paper show the dynamic behavior of the leading-edge vortices on a slender delta wing undergoing a wing rock oscillation. As expected, the dynamic vortex trajectories differed from the static trajectories. For a given roll angle, the dynamic positions of the vortices were found to depend upon the direction of the rolling motion. When the wing was rolling toward a given leading-edge vortex, the vortex was observed to be closer to the wing surface than when the wing was rolling away from the vortex. Differences were also observed in the behavior of vortex breakdown between the static dynamic cases. The motion of the model appears to delay breakdown.

Although these experiments were limited in scope, they do show the differences between the static and dynamic behaviors of the leading-edge vortices in a rolling motion. In the future, it is hoped that experiments can be performed to determine both the dynamic forces and moments acting on the model in conjunction with vortex flow trajectory data. The combination of the force and flowfield data will provide a basis for developing improved theories for the wing rock phenomenon.

Acknowledgments

This research was supported in part by NASA Langley Research Center under Grant NAG-1-727 and the University of Notre Dame. The authors wish to thank Dr. Francis M. Payne for his assistance in obtaining the experimental data.

References

[1]Ross, A. J., "Investigation of Nonlinear Motion Experienced on a Slender-Wing Research Aircraft," *Journal of Aircraft*, Vol. 9, Sept. 1972, pp. 625–631.

[2]Schmidt, L. V., "Wing Rock Due to Aerodynamic Hysteresis," *Journal of Aircraft*, Vol. 16, March 1979, pp. 129–133.

[3]Hui, W. H. and Tobak, M., "Bifurcation Theory Applied to Aircraft Motions," NASA Technical Memorandum 86704, March 1985.

[4]Schiff, L. B. and Tobak, M., "Some Applications of Aerodynamic Formulations to Problems in Aircraft Dynamics," *Dynamic Stability Parameters*, AGARD LS-114, May 1981.

[5]Ericsson, L. E., "The Fluid Mechanics of Slender Wing Rock," *Journal of Aircraft*, Vol. 21, May 1984, pp. 322–328.

[6]Polhamus, E. C., "Prediction of Vortex-Lift Characteristics by Leading Edge Suction Analogy," *Journal of Aircraft*. Vol. 8, April 1971, pp. 193–199.

[7]Nguyen, L. T., Yip, L., and Chamber, J. R., "Self-induced Wing Rock of Slender Delta Wings," AIAA Paper 81-1883, Aug. 1981.

[8]Levin, D. and Katz, J., "Dynamic Load Measurements with Delta Wings Undergoing Self-Induced Roll Oscillation," *Journal of Aircraft*, Vol. 21, Jan. 1984, pp. 30–36.

[9]Jun, Y.-W. and Nelson, R. C., "Leading Edge Vortex Dynamics on a Delta Wing Undergoing a Wing Rock Motion," AIAA Paper 87-0332, Jan. 1987.

[10]Konstadinopoulos, P., Mook, D. T., and Nayfeh, A. H., "Subsonic Wing Rock of Slender Delta Wings," *Journal of Aircraft*, Vol. 22, March 1985, pp. 223–228.